Improved version of a simplified method for including tensor effects in cluster models

N. Itagaki[1] and A. Tohsaki[2]

[1]*Yukawa Institute for Theoretical Physics, Kyoto University, Kitashirakawa Oiwake-Cho, Kyoto 606-8502, Japan*

[2]*Research Center for Nuclear Physics (RCNP), Osaka University, 10-1 Mihogaoka, Ibaraki, Osaka 567-0047, Japan*

(Received 26 June 2017; revised manuscript received 19 October 2017; published 12 January 2018)

The tensor contribution can be directly incorporated in the cluster model in a simplified way. In conventional α cluster models, the contribution of the noncentral interactions exactly cancels because of the antisymmetrization effect and spatial symmetry of α clusters. The mixing of breaking components of α clusters to take into account the spin-orbit and tensor effects is needed. Previously, we proposed a simplified method to include the spin-orbit effect, and also for the tensor part, a simplified model to directly take into account the contribution of the tensor interaction (called SMT) was introduced; however, the contribution of the tensor interaction was quite limited. Here we improve SMT, which is called *i*SMT. Using newly proposed *i*SMT, the contribution of the tensor interaction in ^{4}He is more than -40 MeV, four times larger than the previous version. The method is applied to four-α cluster structure of ^{16}O. In ^{16}O, the tensor contribution is also large, and this is coming from the finite size effect for the distances among α clusters with a tetrahedral configuration.

DOI: 10.1103/PhysRevC.97.014304

I. INTRODUCTION

The binding energy per nucleon of ^{4}He is quite large in light mass region and α particles are considered as good building blocks for the nuclear structure. Cluster models, especially the α cluster models, are based on this idea, and they have been widely used for the description of molecular structure of nuclei [1,2]. One of the well-known examples is the so-called Hoyle state [3]; formation of ^{12}C from three ^{4}He nuclei (α clusters) is a key process of the nucleosynthesis. The second 0^+ state at $E_x = 7.6542$ MeV plays a crucial role, which is the second excited state of ^{12}C and located just above the threshold energy to decay into three ^{4}He nuclei. The existence of a state that has the character of three α clusters just at this energy is really an essential factor in the synthesis of various elements in stars. Such three-α-state is described by various cluster models, and among them, the Tohsaki-Horiuchi-Schock-Röpke (THSR) wave function is a powerful tool to describe gaslike cluster states with spatial extension [4]. Based on the shell-model picture, which is standard in nuclear structure physics, we often need large model space to describe cluster states. Since some of the nucleons are spatially correlated around the nuclear surface, the cluster states are difficult to be described with a framework in which the wave function of each nucleon is expanded around the origin. Therefore, the cluster structures are challenges of the shell models, including modern *ab initio* ones [5–7].

Nuclear systems have characteristic features that noncentral interactions play a crucial role; however, in most of the cluster models, the spin-orbit and tensor interactions do not contribute inside α clusters and also between α clusters because of the antisymmetrization effect and spatial symmetry of α cluster. In cluster models, each α cluster is often defined as a simple $(0s)^4$ configuration at some spatial point, and α cluster is a spin singlet system, which is free from the noncentral interactions. Concerning the spin-orbit interaction, this is known to be quite important in explaining the observed magic numbers. The jj-coupling shell model, which is the standard model for the nuclear structure, is based on this picture.

Our goal is to pave the way to generally describe the nuclear structure, including shell and cluster structures simultaneously. Here, contrary to the standard approaches, we start with the cluster model side and try to include shell correlations. This is because our approach requires much less computational efforts compared with the case starting with the shell model side. To include the spin-orbit contribution starting with the cluster model, we proposed the antisymmetrized quasicluster model (AQCM) [8–16], which allows smooth transition of α cluster model wave function to jj-coupling shell model one. In AQCM, this transition can be controlled by only two parameters: R representing the distance between α clusters and Λ, which characterizes the transition of α cluster(s) to jj-coupling shell model wave functions and quantifies the role of the spin-orbit interaction. We call the transformed α clusters in this way quasiclusters. As it is well known, the conventional α cluster models cover the model space of closure of major shells ($N = 2$, $N = 8$, $N = 20$, etc.), and in addition, the subclosure configurations of the jj-coupling shell model, $p_{3/2}$ ($N = 6$), $d_{5/2}$ ($N = 14$), $f_{7/2}$ ($N = 28$), and $g_{9/2}$ ($N = 50$) can be described by our AQCM. In this way, the cluster and jj-coupling shell model wave functions can be described on the same footing, and the spin-orbit interaction, which is the rank one noncentral interaction, can be successfully taken into account in the cluster model.

However, the rank two noncentral interaction, the tensor interaction, is more complicated to be treated in the cluster model. The tensor interaction has two features, the first-order type and the second-order type. The first-order one is rather weak and characterized by the attractive effect for a proton (neutron) with the j-upper orbit of the jj-coupling shell model and a neutron (proton) with j-lower orbit, or repulsive effect

for the j-upper (j-lower) two protons or two neutrons [17]. This effect can be included just by switching on the tensor interaction in the Hamiltonian, after transforming cluster wave function to jj-coupling shell model one using AQCM mentioned above. The second-order effect of the tensor is much stronger. According to the *ab initio* calculations, the (negative) contribution of the tensor interaction in ^{4}He is quite large, more than -65 MeV [18], and this is even more important than the central interaction. Here, it is found that the two particle two hole ($2p2h$) excitation to higher shells, especially to the p shell, is quite important. According to the tensor optimized shell model (TOSM) calculations [19–23], the p orbits of this $2p2h$ states must have very shrunk shape compared with the normal shell model orbits, and this means that mixing of very high momentum components is quite important.

This second-order effect of the tensor interaction is more difficult to be treated in the cluster model, and we need an additional framework; we have proposed a simplified model to directly take into account the contribution of the tensor interaction (SMT) [24]. The tensor contribution was estimated in ^{4}He, ^{8}Be, and ^{12}C, and the relation to the clustering was quantitatively discussed. However, the contribution of the tensor interaction was rather limited, about -10 MeV in the α cluster, and improvement of the model was needed. In our previous SMT, we started with an α cluster with a $(0s)^4$ configuration and expressed deuteronlike excitation of a proton and neutron to higher shells by shifting the values of the Gaussian center parameters of these two particles. However, shifting the positions of Gaussian center parameters may not be enough for the purpose of mixing higher momentum components of $2p2h$ configurations, and this could be the reason. In the present article, we introduce improved version of SMT, which is iSMT. Here, imaginary part of Gaussian center parameters is shifted in stead of the real part. The imaginary part of Gaussian center parameter corresponds to the expectation value of momentum for the nucleon. The tensor interaction has the character which is suited to be described in the momentum space, and this method is considered to be more efficient in directly mixing the higher momentum components of $2p2h$ configurations.

The purpose of the present work is to incorporate the $2p2h$ nature of the tensor contribution in the cluster model in a simplified and more efficient way compared with the previous SMT. We improve SMT and newly propose iSMT. First, we apply it to ^{4}He and next discuss that the clustering of four α's is closely related to the tensor effect in ^{16}O. There have been fundamental discussion for the appearance of cluster structure in the 1960s; one-pion exchange potential (OPEP) vanishes in the direct terms when each α cluster is described as a $(0s)^4$ configuration, and this is the reason why inter-cluster interaction is weak. However, it is important to show that clustering is still important, even if the model space is extended and the tensor contributions in each α cluster is taken into account. We discuss that the clustering is enhanced because of the tensor interaction in ^{16}O.

Recently, many other attempts of directly taking into account the tensor part of the interaction in microscopic cluster models have begun. For instance, by combining unitary correlation method (UCOM) and Fermionic molecular dynamics (FMD) [25–27], or using antisymmetrized molecular dynamics (AMD) [28], cluster structure has been extensively studied. In UCOM, the tensor contribution can be taken into account by unitary transforming the Hamiltonian, where two-body correlator is introduced in the exponent of the unitary operator. If we expand this power based on the cluster expansion method, in principle, the Hamiltonian contains may-body operators up to A (mass number) body, thus the truncation of the model space is required. Our strategy is slightly different. Although the framework is phenomenological, we do not perform the unitary transformation of the Hamiltonian, and we introduce an effective model wave function to directly take into account the tensor effect.

For the central part of the interaction, we use the Tohsaki interaction, which has finite-range three-body terms [29]. This interaction is a phenomenological one and designed to reproduce the α-α scattering phase shift. Also it gives reasonable size and binding energy of the α cluster, which is rather difficult in the case of the zero-range three-body interaction, and the binding energy is less sensitive to the choice of size parameter of Gaussian-type single particle wave function. Furthermore, the saturation property is reproduced rather satisfactorily.

II. THE MODEL

A. Hamiltonian

The Hamiltonian ($\hat{H}$) consists of kinetic energy ($\hat{T}$) and potential energy ($\hat{V}$) terms,

$$\hat{H} = \hat{T} + \hat{V}, \tag{1}$$

and the kinetic energy term is described as one-body operator,

$$\hat{T} = \sum_i \hat{t}_i - T_{\rm cm}, \tag{2}$$

and the center of mass kinetic energy ($T_{\rm cm}$), which is constant, is subtracted. The potential energy has central ($\hat{V}_{\rm central}$), spin-orbit ($\hat{V}_{\rm spin\text{-}orbit}$), tensor ($\hat{V}_{\rm tensor}$), and the Coulomb parts.

For the central part of the potential energy ($\hat{V}_{\rm central}$), the Tohsaki interaction is adopted [29], which consists of two-body ($V^{(2)}$) and three-body ($V^{(3)}$) terms:

$$\hat{V}_{\rm central} = \frac{1}{2}\sum_{i\neq j} V^{(2)}_{ij} + \frac{1}{6}\sum_{i\neq j, j\neq k, i\neq k} V^{(3)}_{ijk}, \tag{3}$$

where $V^{(2)}_{ij}$ and $V^{(3)}_{ijk}$ consist of three terms with different range parameters,

$$V^{(2)}_{ij} = \sum_{\alpha=1}^{3} V^{(2)}_{\alpha} \exp\left[-(\vec{r}_i - \vec{r}_j)^2/\mu_\alpha^2\right]\left(W^{(2)}_\alpha + M^{(2)}_\alpha P^r\right)_{ij}, \tag{4}$$

$$V^{(3)}_{ijk} = \sum_{\alpha=1}^{3} V^{(3)}_{\alpha} \exp\left[-(\vec{r}_i - \vec{r}_j)^2/\mu_\alpha^2 - (\vec{r}_i - \vec{r}_k)^2/\mu_\alpha^2\right] \times \left(W^{(3)}_\alpha + M^{(3)}_\alpha P^r\right)_{ij}\left(W^{(3)}_\alpha + M^{(3)}_\alpha P^r\right)_{ik}. \tag{5}$$

Here, P^r represents the exchange of spatial part of the wave functions of interacting two nucleons. In this article, we use F1′ parameter set [15], which was designed to avoid small overbinding of ^{16}O when the original F1 parameter set is

adopted. The difference of F1 and F1′ is only for the three-body Majorana exchange parameter for the shortest range.

For the spin-orbit part, G3RS [30], which is a realistic interaction originally determined to reproduce the nucleon-nucleon scattering phase shift, is adopted:

$$\hat{V}_{\text{spin-orbit}} = \frac{1}{2}\sum_{i\neq j} V_{ij}^{ls}, \tag{6}$$

$$V_{ij}^{ls} = V_{ls}\left[e^{-d_1(\vec{r}_i-\vec{r}_j)^2} - e^{-d_2(\vec{r}_i-\vec{r}_j)^2}\right]P(^3O)\vec{L}\cdot\vec{S}. \tag{7}$$

For the strength, $V_{ls} = 1800$ MeV has been suggested to reproduce the various properties of ^{12}C [15], and we use this value.

Up to this point, the interaction is the same as in Ref. [15], and the main purpose of the present article is to switch on the tensor interaction. For the tensor part, we use Furutani interaction [31]. This interaction nicely reproduces the tail region of one pion exchange potential, and the comparison is shown as Fig. 1 in Ref. [24].

B. Wave function

The single particle wave function has a Gaussian shape [1],

$$\phi_i = \left(\frac{2\nu}{\pi}\right)^{\frac{3}{4}} \exp[-\nu(\boldsymbol{r}_i - \boldsymbol{R}_i)^2]\eta_i, \tag{8}$$

where η_i represents the spin-isospin part of the wave function, and $\boldsymbol{R}_i$ is a parameter representing the center of a Gaussian wave function for the ith particle. The size parameter ν is chosen to be 0.25 fm^{-2} for ^{4}He (0.20 fm^{-2} for ^{16}O). In Brink-Bloch wave function, four nucleons in one α cluster share a common and real value for the Gaussian center parameter. Hence, the contribution of the spin-orbit and tensor interactions vanishes.

The wave function of the total system Ψ is antisymmetrized product of these single particle wave functions,

$$\Psi = \mathcal{A}\{\psi_1\psi_2\psi_3\cdots\cdots\psi_A\}, \tag{9}$$

where A is a mass number. The projections onto parity and angular momentum eigenstates can be performed by introducing the projection operators P^J_{MK} and P^π, and these are performed numerically in the actual calculation.

Based on generator coordinate method (GCM), the superposition of different Slater determinants can be done,

$$\Phi = \sum_i c_i P^J_{\text{MK}} P^\pi \Psi_i. \tag{10}$$

Here, $\{\Psi_i\}$ is a set of Slater determinants, and the coefficients for the linear combination, $\{c_i\}$, are obtained by solving the Hill-Wheeler equation [1].

C. SMT and *i*SMT

Here we explain how we can incorporate the tensor effect starting with the α cluster model. Previously, we have introduced SMT [24]. In SMT, we started with an α cluster with a $(0s)^4$ configuration and changed it for the purpose of including the tensor contribution. For the $(0s)^4$ configuration, the Gaussian center parameter [$\vec{R}$ in Eq. (8)] for the spin-up proton ($\vec{R}_{p\uparrow}$), spin-down proton ($\vec{R}_{p\downarrow}$), spin-up neutron ($\vec{R}_{n\uparrow}$), and spin-down neutron ($\vec{R}_{n\downarrow}$) were all set to zero. In SMT, we mimicked deuterons, where a proton and a neutron have aligned spin orientation and spatially displaced in this spin orientation. For ^{4}He, we transformed it to two deuterons with spin up and down; we shifted the Gaussian center of the spin-up proton to the z direction, which forms a deuteron together with the spin-up neutron at the origin, and we also shifted the spin-down neutron to the $-z$ direction, which forms a deuteron with the spin-down proton at the origin. The Gaussian center parameters were introduced in the following way:

$$\vec{R}_{p\uparrow} = d\vec{e}_z, \quad \vec{R}_{n\uparrow} = 0,$$
$$\vec{R}_{p\downarrow} = 0, \quad \vec{R}_{n\downarrow} = -d\vec{e}_z, \tag{11}$$

where d is a distance parameter and $\vec{e}_z$ is a unit vector for the z direction. We prepared Slater determinants with different d values and superposed them based on GCM. The adopted d values in Ref. [24] were 0, 0.7, 1.4, 2.1, $\cdots$ 7.0 fm (11 Slater determinants in total). When d is 0, the basis state corresponds to the $(0s)^4$ configuration. With increasing d values, $2p2h$ excitation to higher shell mixes, but we can show that components of one particle one hole ($1p1h$) also mixes when we expand the power of the exponents of the single-particle wave function in Eq. (8).

However, using this previous version of SMT, the contribution of the tensor interaction was rather limited, about -10 MeV in the α cluster. Shifting the positions of Gaussian center parameters may not be enough for the purpose of mixing higher momentum components of $2p2h$ configurations, and this could be the reason why the effect of the tensor interaction was rather limited. According to TOSM, the higher-nodal orbits of the $2p2h$ states must be introduced to have very shrunk shape compared with the normal shell model orbits. In Fig. 1,

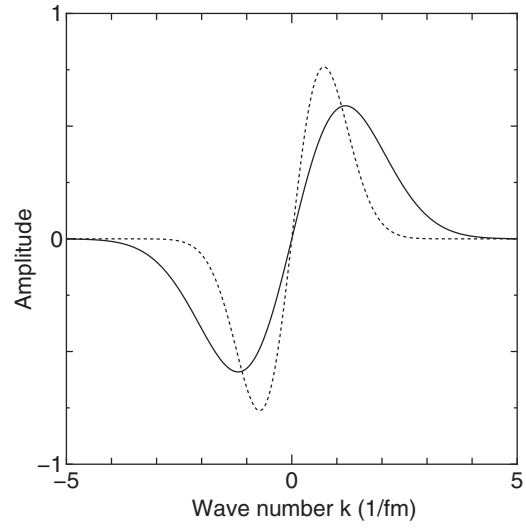

FIG. 1. Fourier transformation of the p orbit (one dimension). The horizontal axis is the wave number k (fm^{-1}). The dotted line is is for the normal p orbit with the standard size parameter ($b = 1.4$ fm), and the solid line is the one used in TOSM with a shrunk size parameter ($b = 0.6 \times 1.4$ fm).

Fourier transformation of one dimensional p orbit is shown. The p orbit on the x axis before the Fourier transformation is proportional to $x\exp[-\nu x^2]$, and $\nu = 1/2b^2$. The horizontal axis is the wave number k (fm^{-1}). The dotted line is for the normal p orbit after the Fourier transformation with the standard size parameter ($b = 1.4$ fm), and the solid line is the one used in TOSM (solid line) with a shrunk size parameter ($b = 0.6 \times 1.4 = 0.84$ fm). After the Fourier transformation, the shrinkage in the coordinate space changes to the extension in the the momentum space; the solid line is distributed in much larger $|k|$ region compared with the dotted line. The root mean square of k is 1.46 (fm^{-1}) and 0.87 (fm^{-1}) for the solid and dotted line, respectively.

In the present article, we introduce improved version of SMT, which is iSMT. Here, imaginary part of Gaussian center parameters is shifted in stead of the real part. Using the single particle wave function [Eq. (8)], we can show that the expectation value of the momentum of the nucleon is proportional to the imaginary part of the Gaussian center parameter,

$$\langle \vec{p} \rangle = 2\nu\hbar \mathrm{Im}(\vec{R}). \tag{12}$$

In the present calculation, ν is chosen as 0.25 fm^{-2} for ^{4}He, thus the imaginary part of the Gaussian center parameter and the wave number have the relation of

$$\langle \vec{k} \rangle = 0.5 \times \mathrm{Im}[\vec{R}(\mathrm{fm})] \ (\mathrm{fm}^{-1}). \tag{13}$$

In iSMT, the Gaussian center parameters are introduced in the following way:

$$\vec{R}_{p\uparrow} = di\vec{e}_z, \quad \vec{R}_{n\uparrow} = 0,$$
$$\vec{R}_{p\downarrow} = 0, \quad \vec{R}_{n\downarrow} = -di\vec{e}_z. \tag{14}$$

According to Fig. 1, the shrunk wave function of TOSM contains the components of the wave number k up to 3–4 fm^{-1}. Using the relation shown in Eq. (13), $k = 4$ fm^{-1} corresponds to 8 fm for the imaginary part of the Gaussian center parameter. Therefore, the d values are taken as 0, 1, 2, ... 10 fm (11 Slater determinants). The expectation value of the momentum for $d = 10$ fm is 5 fm^{-1}. In addition, we prepare the basis states, where neutron spin-up is shifted instead of neutron spin-down:

$$\vec{R}_{p\uparrow} = di\vec{e}_z, \quad \vec{R}_{n\uparrow} = -di\vec{e}_z,$$
$$\vec{R}_{p\downarrow} = 0, \quad \vec{R}_{n\downarrow} = 0, \tag{15}$$

and d values are 1, 2, ... 10 fm (10 Slater determinants). Eventually, we superpose these 21 Slater determinants in total based on GCM. Note again that when d is 0, the basis state corresponds to the $(0s)^4$ configuration, and with increasing d values, $2p2h$ excitation to higher shell mixes, but $1p1h$ also mixes, which is shown by expanding the power of the exponents of the single particle wave functions shown in Eq. (8).

III. RESULTS

A. ^{4}He

We start with ^{4}He. The energy convergence for the ground state of ^{4}He described based on iSMT is shown in Fig. 2 as a function of number of basis states. Here iSMT is a linear combination of 21 GCM basis states; the basis state "1" is $(0s)^4$ configuration, and in 2–11 (12–21), the imaginary part of the Gaussian center parameters for the spin-up proton and spin-down (spin-up) neutron are shifted as in Eq. (14) [Eq. (15)], where d values are 1, 2, 3, ... 10 fm. At "1" on the horizontal axis, the tensor interaction does not contribute, and the energy gets lower by more than 20 MeV with increasing the number of the GCM basis states.

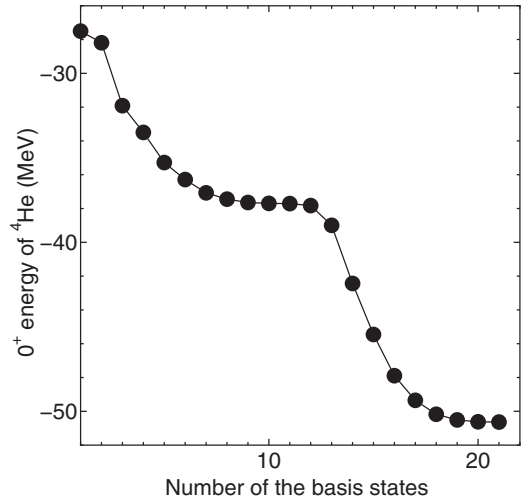

FIG. 2. Energy convergence for the ground state of ^{4}He described based on iSMT as a function of number of basis states.

In Table I, we compare the energies of ^{4}He calculated using the $(0s)^4$ configuration, conventional SMT, and newly introduced iSMT. Here total, T, V^2, V^3, V^{ls}, V^t, and V^{Coul} mean the expectation value of the total energy, kinetic energy, two-body interaction, three-body interaction, spin-orbit interaction, tensor interaction, and Coulomb interaction, respectively. The tensor contribution of iSMT is −41.56 MeV, which is more than four times compared with the previous version. The kinetic energy of iSMT increases from the value for the $(0s)^4$ configuration by about 25 MeV in the positive direction, and

TABLE I. Energies of ^{4}He calculated using the $(0s)^4$ configuration, conventional SMT, and newly introduced iSMT. In the column SMT′, basis states where Gaussian center parameters of spin-up neutron is shifted in stead of spin-down neutron are added to SMT. Here total, T, V^2, V^3, V^{ls}, V^t, and V^{Coul} mean the expectation values of the total energy, kinetic energy, two-body interaction, three-body interaction, spin-orbit interaction, tensor interaction, and Coulomb interaction, respectively. All units are in MeV.

	$(0s)^4$	SMT	iSMT	SMT′
Total	−27.50	−32.85	−50.64	−37.25
T	46.65	53.14	71.96	55.40
V^2	−79.38	−83.75	−88.65	−81.29
V^3	4.41	6.22	6.18	5.07
V^{ls}	0.0	0.11	0.57	0.37
V^t	0.0	−9.40	−41.56	−17.62
V^{Coul}	0.81	0.84	0.87	0.83

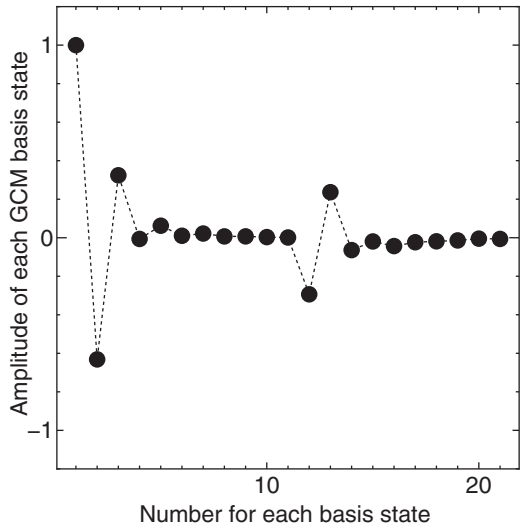

FIG. 3. Amplitude for the linear combination of the basis states [c_i in Eq. (10)] for ^{4}He described based on iSMT. The amplitude for the $(0s)^4$ configuration (basis state 1) is normalized to 1.

this is because of the mixing of higher momentum components. Here we can see that the contribution of the two-body interaction increases by about 9 MeV in the negative direction. Compared with the so called *ab initio* calculations, the tensor contribution is still small, but we can include the effect to the level of −40 MeV (our central part of the interaction is phenomenological one without short range core, thus precise comparison with *ab initio* calculations is rather difficult).

To directly compare SMT and iSMT with the same number of basis states, we introduce SMT′, whose results are shown in the column SMT′. In SMT′, real part of Gaussian center parameters are shifted as in SMT [Eq. (11)], and in addition to the 11 basis states of SMT, 10 basis states where (the real parts of) Gaussian center parameters of the spin-up neutron are shifted in stead of the spin-down neutron are added as in iSMT. The tensor contribution is −17.62 MeV, almost twice the value of SMT, but this is much smaller than in iSMT.

The amplitude for the linear combination of the basis states [c_i in Eq. (10)] for ^{4}He described based on iSMT is shown in Fig. 3. These amplitudes are obtained after superposing 21 basis states of iSMT. The basis state "1" on the horizontal axis corresponds to the $(0s)^4$ configuration, and in the basis states 2–11 (12–21), the imaginary part of the Gaussian center parameters for the spin-up proton and spin-down (spin-up) neutron are shifted as in Eq. (14) [Eq. (15)]. In principle, the amplitudes can be complex numbers; however, here we obtained real numbers after diagonalizing the Hamiltonian. These coefficients are considered to contain the information for the nodes of each resultant single particle wave function. For instance, if we superpose two Gaussians with different central positions and opposite signs for the amplitudes, we can create one-node orbit. However, in this study, we shift the Gaussian center parameters of two particles in each basis state, thus the direct correspondence between the amplitude of each basis state and the resultant single particle orbit is not clear. Nevertheless, in Fig. 3, "1" on the horizontal axis correspond to the amplitude of $(0s)^4$ configuration, which is normalized to 1. In the basis "2," the dominant component is still the $(0s)^4$ configuration; however new components, where (a) two particles are excited to the p shell and (b) one particle is excited to the sd shell, are mixed (here we focus on the positive parity states). The negative sign for the coefficient of basis state "2" indicates the reduction of the $(0s)^4$ component. As for the mixing of two particle excitation to the p shell, in principle even higher shells are already mixed, but the shift of Gaussian center parameters is not yet large in "2" and at this stage we have only two Slater determinants to be superposed, thus the dominant excitation may be the lowest order one, which is the excitation to the p shell. As for the excitation of one particle to the sd shell, in the present case of ^{4}He, other three nucleons occupy s-orbit, and the component of excitation of one nucleon to d-orbit vanishes after the angular momentum projection to 0^+. However, if the core nucleus has more complicated configuration such as the tetrahedron configuration of four α clusters in ^{16}O, which will be discussed later, the excitation to the d-orbit also contributes even after the angular momentum projection to 0^+, since the core nucleus can have the components of finite angular momentum. The basis state "3" with larger shift for the Gaussian center parameters has the amplitude with positive sign. The amplitude and the sign are considered to be determined so as to optimize the mixing ratio of three components, $(0s)^4$, $2p2h$ to p orbit, and $1p1h$ to higher s orbit. With increasing number of basis states, the shift of the Gaussian center parameters gets larger. Thus, although the absolute value of the amplitude becomes smaller, the particle-hole excitation to even higher shells is mixed. From "12," spin-up neutron is shifted in stead of spin-down neutron. Although the absolute value of the amplitude is smaller, the basic tendency is the same as the spin-down neutron case.

TABLE II. Physical quantities of ^{4}He calculated using conventional SMT and newly introduced iSMT. Here n, one-body ls, and $(0s)^4$ mean the expectation values of principal quantum number, one-body spin-orbit operator, and the component of $(0s)^4$ configuration, respectively. In the column SMT′, basis states where real parts of Gaussian center parameters of spin-up neutron are shifted in stead of spin-down neutron are added to SMT.

	SMT	iSMT	SMT′
n	0.21	0.85	0.37
one-body ls	−0.012	−0.053	−0.040
$(0s)^4$	0.96	0.89	0.94

In Table II, we show the squared overlaps between the obtained ground state of ^{4}He with the tensor contribution and the $(0s)^4$ configuration. The value is 0.89 in the case of new iSMT. Using the old version, SMT, the value is 0.96. Thus, the mixing of particle-hole configurations is much enhanced in iSMT, and the matrix element of tensor interaction is four times stronger in iSMT as already mentioned. However, according to the TOSM+UCOM calculation [22], this value is 0.89, and more particle-hole configurations should be mixed. This is the reason why our matrix element of tensor is still −40 MeV level

and not −60 MeV level in *ab initio* calculations. It is considered that more complex configurations should be mixed.

In Table II, the expectation values of the principal quantum number n of the harmonic oscillator are also shown. The value increased from 0.21 in SMT to 0.85 in iSMT. Thus more particle configurations are mixed in iSMT. It is worthwhile to mention that 90% of the wave function is the simple $(0s)^4$ configuration, and when the remaining 10% of the wave function is the $2p2h$ excitation to the p shell, the expectation value of the principal quantum number should be 0.2. Therefore, the expectation value of 0.85 means that the excitation of nucleons to much higher shells are mixed. The values of SMT′ are also listed, and they are just in between SMT and iSMT.

In Table II, we also list the expectation values of one-body spin-orbit operator, $\sum_i \mathbf{l}_i \cdot \mathbf{s}_i$. The α cluster model wave function gives zero for this operator, and the components of nucleons in the jj-coupling shell model gives finite values. For instance, a nucleon in $p_{3/2}$, $p_{1/2}$, $d_{5/2}$, $d_{3/2}$, and $f_{7/2}$ gives the eigen values of 0.5, −1.0, 1.0, −1.5, and 1.5, respectively. Here, the negative expectation value is obtained for ^{4}He, and this indicates that the excitation of nucleons to j-lower orbit, including $p_{1/2}$, is important (however, note that if the same amount of $(p_{3/2})^2$ and $(p_{1/2})^2$ components are mixed, the expectation value of one-body spin-orbit operator becomes also negative because of the difference of the eigen values).

B. ^{16}O

The same procedure can be applied to ^{16}O and we can discuss the relation between the tensor contribution and the clustering effect. Here, ^{16}O is introduced as a tetrahedral configuration of four-α clusters, and one of the clusters is deformed using iSMT to include the tensor contribution. In the previous case of ^{4}He, the transformation of iSMT in Eqs. (14) and (15) are applied to an α cluster at the origin of the coordinate space; however here the origin of this transformation is moved to the spatial position of one of α clusters. The 0^+ state energy of ^{16}O with a tetrahedral configuration of four-α clusters as a function of distance between α-α is shown in Fig. 4. The solid and dotted lines show the results with and without the tensor interaction. We can confirm that with the tensor interaction, the clustering is even enhanced. The decrease of the energy after switching on the tensor interaction is only 5.7 MeV at the α-α distance of 0.1 fm. Here the contribution of the tensor interaction in the Hamiltonian is only −10.2 MeV. The tensor contribution is suppressed at small relative distances (the wave function corresponds to the closed shell configuration of the p shell at the zero-distance limit). This is because, the $2p2h$ excitation from the lowest s shell to the p shell is forbidden, even though the excitation from the p shell to sd shell is allowed. With increasing the α-α distance, the decrease of the energy due to the tensor interaction is enhanced. The decrease is about 20 MeV around the lowest energy point, and the matrix element of the tensor interaction is −32.7 MeV at the α-α distance of 2 fm. Therefore, it can be concluded that the tensor interaction has a certain effect for the stability of clusterized configurations. In Refs. [32,33], it has been suggested that tensor contribution is suppressed in ^{16}O, since $2p2h$ excitation

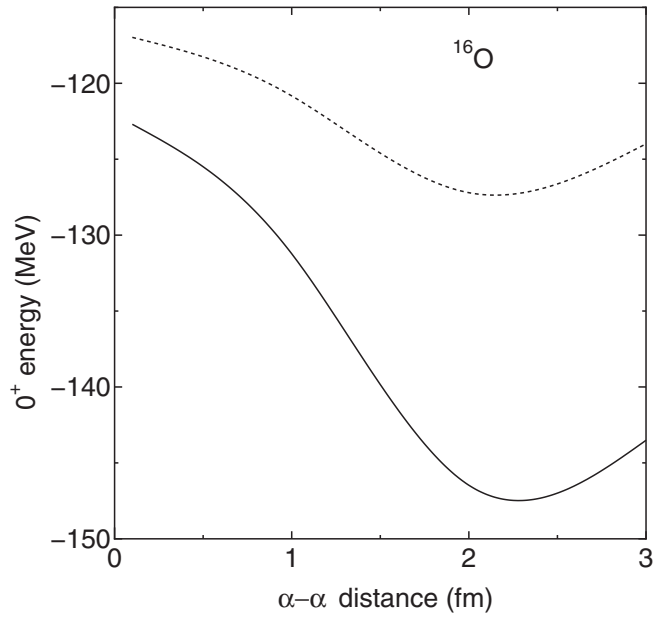

FIG. 4. Energy curve for the 0^+ state of ^{16}O with a tetrahedral configuration of four-α clusters as a function of the α-α distance. The solid and dotted line show the results with and without the tensor interaction.

from the lowest s shell to the p shell is forbidden at the shell model limit. This is true; however, tensor contribution turns out to be large in ^{16}O because of the clustering effect of four α's.

Similarly to ^{4}He, for ^{16}O, the expectation value of the one-body spin-orbit operator as a function of α-α distance is shown in Fig. 5. The value is almost constant between 0.5 and 0.6. Even at the zero limit for the α-α distance, the value is almost constant. At this limit, four alpha cluster wave function corresponds to the doubly closed configuration of the p shell, and all the single particle orbits up to p shell

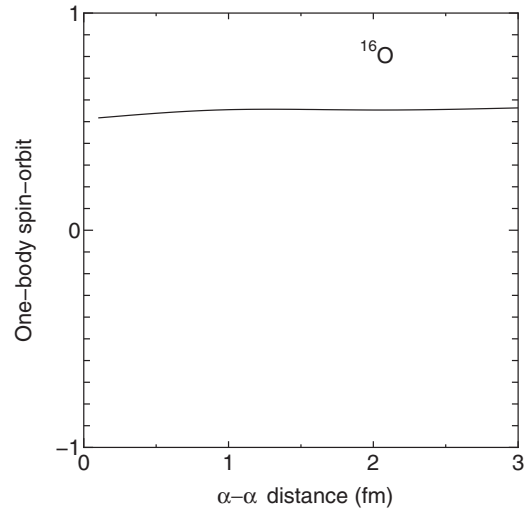

FIG. 5. Expectation value of the one-body spin-orbit operator $\sum_i \mathbf{l}_i \cdot \mathbf{s}_i$ for ^{16}O as a function of the α-α distance.

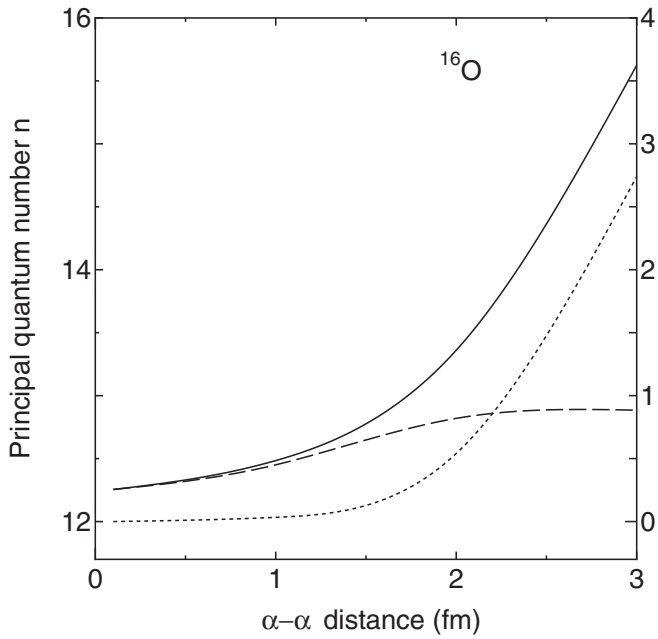

FIG. 6. Principal quantum number n of harmonic oscillator for ^{16}O as a function of the α-α distance. The dotted line shows the value for the tetrahedron configuration of four α clusters, and the solid line shows the one after introducing iSMT. The difference between these two shows the effect of iSMT (dashed line), which corresponds to the right vertical axis.

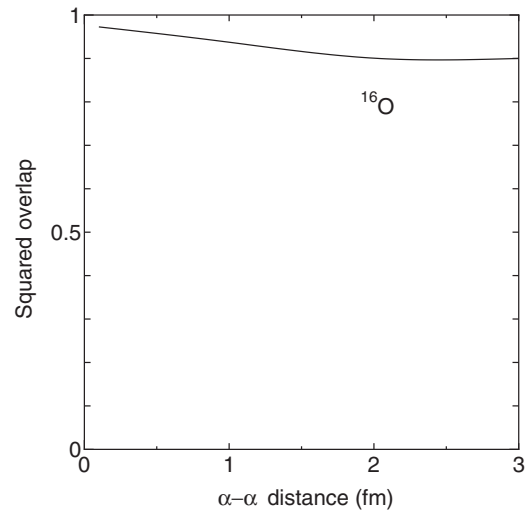

FIG. 7. Squared overlap of ^{16}O between the result of iSMT and tetrahedron configuration of four α clusters for each α-α distance.

are occupied. Thus, here, the iSMT transformation works to describe the particle-hole excitation from p shell to unoccupied higher shell, owing to the antisymmetrization effect. Contrary to ^{4}He, the expectation value of one-body spin-orbit operator has a positive sign, since both the reduction of the $p_{1/2}$ component and increase of $d_{5/2}$ component contribute in the positive direction. With increasing α-α distance, the particle-hole excitation from the lowest s shell to p shell starts working; however the contribution to the one-body spin-orbit value is small as shown in the ^{4}He case.

The expectation value of the principal quantum number is shown in Fig. 6. Here, the dotted line shows the value for the tetrahedron configuration of four α clusters, and the solid line shows the one after introducing iSMT. The difference between these two shows the particle-hole excitation related to the tensor interaction (dashed line), which corresponds to the right vertical axis. Again the particle-hole excitation is not zero at the zero limit of the α-α distance, and the difference of two lines increase around the α-α distance of 1–2 fm. This is because particle-hole excitation from the lowest s shell to higher shells, which is important in ^{4}He, becomes possible.

Finally, the squared overlap between the result of iSMT and tetrahedron configuration of four α clusters for each α-α distance is shown in Fig. 7. The squared overlap decreases with increasing α-α distance and becomes almost constant around the distance of 2 fm. There the squared overlap is around 0.9, which means the breaking of four-α cluster model is about 10%, similarly to the case of ^{4}He.

In the present case, this $2p2h$ tensor effect is already renormalized in the central part of the effective interaction as in many conventional models, and the result gives very large overbinding. In the next step, the modification of the central part of the two-body and three-body interactions to reproduce the binding energies of many nuclei including this kind of tensor effect will be carried out.

IV. SUMMARY

It has been shown that the tensor contribution can be incorporated in the cluster model in a simplified way. In conventional α cluster models, the contribution of the noncentral interactions cancels because of the antisymmetrization effect and spatial symmetry of each α cluster, and the mixing of the breaking components of α clusters to take into account the spin-orbit and tensor effects is needed. Previously we proposed a simplified method to include the spin-orbit effect, and also for the tensor part, a simplified method to take into account the tensor contribution in the cluster model (SMT) was introduced. Here we improved SMT, which is called iSMT, where the imaginary part of Gaussian center parameters of nucleons in one α cluster was shifted in stead of the real part. The imaginary part of Gaussian center parameter corresponds to the expectation value of momentum for the nucleon. The tensor interaction has the character which is suited to be described in the momentum space, and this method is considered to be more efficient in directly mixing the higher momentum components of $2p2h$ configurations.

Using newly proposed iSMT, the contribution of the tensor interaction in ^{4}He is more than -40 MeV, four times larger than the previous version. The method was applied to four-α-cluster structure of ^{16}O. In ^{16}O, the tensor contribution is suppressed at the limit of small relative distance corresponding to the closed shell configuration of the p shell. With increasing the α-α distance, the decrease of the energy due to the tensor interaction is enhanced; about 20 MeV around the lowest energy point. Therefore, it can be concluded that the tensor interaction has a certain effect for the stability of clusterized configurations.

In the present case, this $2p2h$ tensor effect is already renormalized in the central part of the effective interaction as in many conventional models, and the result gives very large overbinding. As a future work, we modify the central part of the two-body and three-body interactions to reproduce the binding energies of many nuclei including this kind of tensor effect.

ACKNOWLEDGMENTS

Numerical calculation has been performed using the computer facility of Yukawa Institute for Theoretical Physics, Kyoto University. This work was supported by JSPS KAKENHI Grant-in-Aid for Scientific Research (C), Grant No. 17K05440.

[1] D. M. Brink, in *Proceedings of the International School of Physics "Enrico Fermi" Course XXXVI*, edited by C. Bloch (Academic Press, New York, 1966), p. 247.
[2] Y. Fujiwara *et al.*, Suppl. Prog. Theor. Phys. **68**, 29 (1980).
[3] F. Hoyle, D. N. F. Dunbar, W. A. Wenzel, and W. Whaling, Phys. Rev. **92**, 1095c (1953).
[4] A. Tohsaki, H. Horiuchi, P. Schuck, and G. Röpke, Phys. Rev. Lett. **87**, 192501 (2001).
[5] P. Maris, J. P. Vary, and A. M. Shirokov, Phys. Rev. C **79**, 014308 (2009).
[6] A. C. Dreyfussa, K. D. Launeyb, T. Dytrychb, J. P. Draayerb, and C. Bahri, Phys. Lett. B **727**, 511 (2013).
[7] T. Yoshida, N. Shimizu, T. Abe, and T. Otsuka, J. Phys.: Conf. Ser. **569**, 012063 (2014).
[8] N. Itagaki, H. Masui, M. Ito, and S. Aoyama, Phys. Rev. C **71**, 064307 (2005).
[9] H. Masui and N. Itagaki, Phys. Rev. C **75**, 054309 (2007).
[10] T. Yoshida, N. Itagaki, and T. Otsuka, Phys. Rev. C **79**, 034308 (2009).
[11] N. Itagaki, J. Cseh, and M. Płoszajczak, Phys. Rev. C **83**, 014302 (2011).
[12] T. Suhara, N. Itagaki, J. Cseh, and M. Płoszajczak, Phys. Rev. C **87**, 054334 (2013).
[13] T. Suhara and Y. Kanada-En'yo, Phys. Rev. C **91**, 024315 (2015).
[14] N. Itagaki, H. Matsuno, and T. Suhara, Prog. Theor. Exp. Phys. (2016) 093D01.
[15] N. Itagaki, Phys. Rev. C **94**, 064324 (2016).
[16] H. Matsuno, N. Itagaki, T. Ichikawa, Y. Yoshida, and Y. Kanada-En'yo, Prog. Theor. Exp. Phys. (2017) 063D01.
[17] T. Otsuka, T. Suzuki, R. Fujimoto, H. Grawe, and Y. Akaishi, Phys. Rev. Lett. **95**, 232502 (2005).
[18] H. Kamada, A. Nogga, W. Glöckle, E. Hiyama, M. Kamimura, K. Varga, Y. Suzuki, M. Viviani, A. Kievsky, S. Rosati, J. Carlson, S. C. Pieper, R. B. Wiringa, P. Navrátil, B. R. Barrett, N. Barnea, W. Leidemann, and G. Orlandini, Phys. Rev. C **64**, 044001 (2001).
[19] T. Myo, K. Katō, and K. Ikeda, Prog. Theor. Phys. **113**, 763 (2005).
[20] T. Myo, S. Sugimoto, K. Katō, H. Toki, and K. Ikeda, Prog. Theor. Phys. **117**, 257 (2007).
[21] T. Myo, H. Toki, and K. Ikeda, Prog. Theor. Phys. **121**, 511 (2009).
[22] T. Myo, A. Umeya, H. Toki, and K. Ikeda, Phys. Rev. C **84**, 034315 (2011).
[23] T. Myo, A. Umeya, H. Toki, and K. Ikeda, Phys. Rev. C **86**, 024318 (2012).
[24] N. Itagaki, H. Masui, M. Ito, S. Aoyama, and K. Ikeda, Phys. Rev. C **73**, 034310 (2006).
[25] T. Neff and H. Feldmeier, Nucl. Phys. A **738**, 357 (2004).
[26] R. Roth, T. Neff, and H. Feldmeier, Prog. Part. Nucl. Phys. **65**, 50 (2010).
[27] M. Chernykh, H. Feldmeier, T. Neff, P. von Neumann-Cosel, and A. Richter, Phys. Rev. Lett. **98**, 032501 (2007); **105**, 022501 (2010).
[28] A. Doté, Y. Kanada-En'yo, H. Horiuchi, Y. Akaishi, and K. Ikeda, Prog. Theor. Phys. **115**, 1069 (2006).
[29] A. Tohsaki, Phys. Rev. C **49**, 1814 (1994).
[30] R. Tamagaki, Prog. Theor. Phys. **39**, 91 (1968).
[31] H. Furutani, H. Horiuchi, and R. Tamagaki, Prog. Theor. Phys. **60**, 307 (1978).
[32] Y. Ogawa, H. Toki, S. Tamenaga, S. Sugimoto, and K. Ikeda, Phys. Rev. C **73**, 034301 (2006).
[33] Y. Ogawa and H. Toki, Nucl. Phys. **860**, 22 (2011).